Earth and Planetary Science Letters 357-358 (2012) 238–248

Contents lists available at SciVerse ScienceDirect

Earth and Planetary Science Letters

journal homepage: www.elsevier.com/locate/epsl

Effect of fluid circulation on subduction interface tectonic processes: Insights from thermo-mechanical numerical modelling

S. Angiboust [a,c,*], S. Wolf [a], E. Burov [a], P. Agard [a], P. Yamato [b]

[a] ISTEP 46-00, 3e case 129, UMR CNRS 7193, UPMC Sorbonne Universités, F-75252 Cedex 05, Paris, France
[b] Geosciences Rennes, UMR CNRS 6118, Université de Rennes1 Campus Beaulieu CS 74205, F-35 042 Rennes Cedex, France
[c] Helmholtz-Zentrum – Deutsches GeoForschungsZentrum, Telegrafenberg, D-14473 Potsdam, Germany

ARTICLE INFO

Article history:
Received 25 April 2012
Received in revised form
7 September 2012
Accepted 12 September 2012
Editor: T. Spohn
Available online 23 October 2012

Keywords:
numerical modelling
fluids
subduction
exhumation

ABSTRACT

Both geophysical and petrological data suggest that large amounts of water are released in subduction zones during the burial of oceanic lithosphere through metamorphic dehydration reactions. These fluids are generally considered to be responsible for mantle wedge hydration, mechanical weakening of the plate interface and to affect slab-interface seismicity. In order to bridge the gap between subduction dynamics and the wealth of field, petrological and experimental data documenting small-scale fluid circulation at mantle depths, we designed a bi-phase model, in which fluid migration is driven by rock fluid concentrations, non-lithostatic pressure gradients and deformation. Oceanic subduction is modelled using a forward visco-elasto-plastic thermo-mechanically and thermodynamically coupled code (FLAMAR) following the previous work by Yamato et al. (2007). After 16.5 Myr of convergence, deformation is accommodated along the subduction interface by a low-strength shear zone characterised by a weak (10–25% of serpentinite) and relatively narrow (5–10 km) serpentinized front in the reference experiment. Dehydration associated with eclogitization of the oceanic crust (60–75 km depth) and serpentinite breakdown (110–130 km depth) significantly decreases the mechanical strength of the mantle at these depths, thereby favouring the detachment of large slices of oceanic crust along the plate interface. The geometries obtained are in good agreement with reconstructions derived from field evidence from the Alpine eclogite-facies ophiolitic belt (i.e., coherent fragments of oceanic crust detached at ca.80 km depth in the Alpine subduction zone and exhumed along the subduction interface). Through a parametric study, we further investigate the role of various parameters, such as fluid circulation, oceanic crustal structure and rheology, on the formation of such large tectonic slices. We conclude that the detachment of oceanic crust slices is largely promoted by fluid circulation along the subduction interface and by the subduction of a strong and originally discontinuous mafic crust.

1. Introduction and geological constraints

An increasing number of geophysical (Hebert et al., 2009; Kuge et al., 2010; Gerya and Meilick, 2011; van Keken et al., 2011), petrological (Bachmann et al., 2009; Padron-Navarta et al., 2010) and experimental studies (Hilairet and Reynard, 2009; Kawano et al., 2011) confirmed the fundamental role of fluids on intermediate depths interplate rheological and mechanical subduction processes.

Prior to subduction, huge amounts of water are also added to the oceanic lithosphere by hydrothermal alteration and/or downward percolation of seawater through fractures in the bending lithosphere entering trenches (Watts et al., 1980; McAdoo and Martin, 1984; Burov and Diament, 1995; Rüpke et al., 2004). During subduction, dehydration reactions accompanying prograde metamorphism transfer part of these fluids to the Earth mantle: (1) to the upper plate mantle wedge, ultimately causing arc magmatism and affecting subduction zone rheology and mechanical coupling along the plates interface (Iwamori, 1998; Oncken et al., 1999; Peacock and Hyndman, 1999; van Keken, 2003; Arcay et al., 2005; Wada et al., 2008; Bachmann et al., 2009), (2) to the upper part of the lower plate oceanic mantle (Schmidt and Poli, 1998; Ranero et al., 2003; Zhang et al., 2004; Faccenda et al., 2009; Contreras-Reyes, Carrizo, 2011; Fig. 1), and beyond (Green et al., 2010).

Such dehydration reactions are considered to be partly responsible for the observed intermediate-depth seismicity in the Wadati–Benioff zone (e.g. Green and Houston, 1995; Peacock, 2001; Hacker et al., 2003), together with hydraulic fracturing and reactivation of inherited faults (Davies, 1999; Rietbrock and

* Corresponding author. Now at GFZ Potsdam, Germany.
Tel.: +49 331 288 1363; fax: +49 331 288 1370.
E-mail address: samuel.angiboust@gmail.com (S. Angiboust).

0012-821X/$ - see front matter © 2012 Elsevier B.V. All rights reserved.
http://dx.doi.org/10.1016/j.epsl.2012.09.012

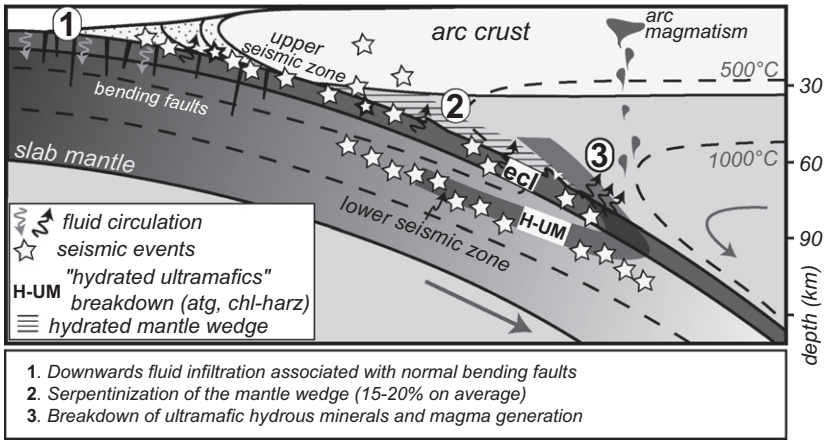

Fig. 1. Schematic view of a typical subduction zone showing the main fluid transfer processes and the location of the recorded seismic events.

Waldhauser, 2004; Angiboust et al., 2012a). The coupling between these prograde dehydration and hydration reactions (such as mantle serpentinization) could also be responsible for the detachment of tens of kilometres long coherent fragments of the downgoing slab, such as those found in the exhumed ophiolitic terranes in the Western Alps (where they detached along crustal-scale shear zones channelising fluids: Angiboust et al., 2009, 2011) or as those imaged by geophysical data on active subduction zones (Singh et al., 2008; Toda et al., 2008).

Geophysical observations notably through low S-velocity zones, seismic anisotropies and high Poisson ratios suggest the existence of a hydrous layer on the top of the subduction interface, between the slab and the mantle wedge (e.g. Kodaira et al., 2004; Abers, 2005; Audet et al., 2009; Jung, 2011; Fig. 1). This layer is however not robustly detectable since its thickness (generally ranging from 2 to 10 km) appears to be at the limits of resolution of seismic studies (Abers, 2005; Hilairet and Reynard, 2009). This hydrous layer is thought to be dominantly composed of serpentinite and, to a lesser extent, of talc and/or brucite (e.g. Peacock and Hyndman, 1999). Heat flux measurements also indicate that, except for some relatively "warm" subduction zones (such as the Cascades or Nankai; van Keken et al., 2011), serpentinization of the mantle wedge should be dominantly restricted to the vicinity of the plate interface (Wada et al., 2008 and references therein) and rarely exceed 20–30% (see Hyndman and Peacock, 2003). The mechanical weakening associated with serpentinization is in particular thought to account for the observed lack of seismicity within the mantle wedge.

Despite this recent wealth of data, constraints on the mechanisms allowing fluid extraction and circulation across and/or along the subduction interface and on their mechanical effect on interplate coupling are still critically lacking (e.g. Miller et al., 2003; Hacker et al., 2003; Wada et al., 2008). We herein attempt to bring additional constraints through thermomechanically and thermodynamically coupled numerical modelling. While Arcay et al. (2005) assumed that fluids released by metamorphic dehydration reactions only migrate upwards, recent works proposed that local gradients in tectonic pressure may strongly control fluid flow at depth in subduction zone environments (Faccenda and Mancktelow, 2010; Faccenda et al., 2012; see also Connolly and Podladchikov, 2004). Based on water contents derived from phase diagrams and tectonic pressure gradients, we herein implement fluid migration in an Alpine-type ocean–continent subduction setting (Yamato et al., 2007). In particular, we propose a methodology that enables reproducing the complex interplay between the rock fluid content and the physical and mechanical rock properties at mantle depths in a subduction environment. This kilometre-scale fluid circulation algorithm permits assessing the spatial extent of fluid migration and evaluating the effect of fluids on interplate mechanical coupling. The associated parametric study enables a better understanding of the key parameters controlling the formation of these large mafic slices along the plate interface in "cold" subduction zone settings. Comparison of numerical modelling results with natural data from exhumed ophiolitic belts provides an opportunity to validate the numerical approach herein followed.

2. Numerical modelling method and model setup

2.1. Thermo-mechanical model description

The numerical code FLAMAR v12 (derived from Paravoz; Poliakov et al., 1993, and based on the FLAC algorithm, Cundall, 1989) has been used in this study to assess the impact of fluid transfer processes on interplate subduction dynamics (more details on the numerical method are available in Burov et al., 2001, Yamato et al., 2007 and in Appendix A in supplementary material). The algorithm accounts for (1) large strains, (2) visco-elasto-plastic rheologies including Mohr–Coulomb failure (faulting) and pressure (P) – temperature (T) strain-rate dependent ductile creep, (3) density and rheology changes due to metamorphic reactions, (4) internal heat sources, and (5) free surface boundary conditions combined with erosion/sedimentation processes. The model setup is similar to the one used in the previous work by Yamato et al. (2007), but with a narrower accretionary wedge and a discontinuous oceanic crust, in order to match the seafloor structure of a slow-spreading ocean, such as for the Tethyan seafloor (Fig. 2a; Western Alps; Lagabrielle and Cannat, 1990; see also Gorczyk et al., 2007 for a close initial seafloor structure). The oceanic crust is composed of flat-lying mafic bodies separated by serpentinized mantle (such as inferred for Western Alps ophiolitic domains; Lagabrielle and Lemoine, 1997, or after geophysical observation; Cannat et al., 1997). We imposed the presence of a 6 km-thick partly serpentinized layer below the oceanic mafic crust in order to match recent numerical models demonstrating the existence of a downgoing serpentinization front in slow-spreading contexts (Iyer et al., 2010 and references therein). Thermal structure, boundary conditions and other fixed parameters are identical to those described by Yamato et al. (2007). Input lithologies, chemical compositions and flow laws for the different materials used in the model are given in Table 1. Density and maximum water contents are updated dynamically as function of pressure–temperature (P–T)

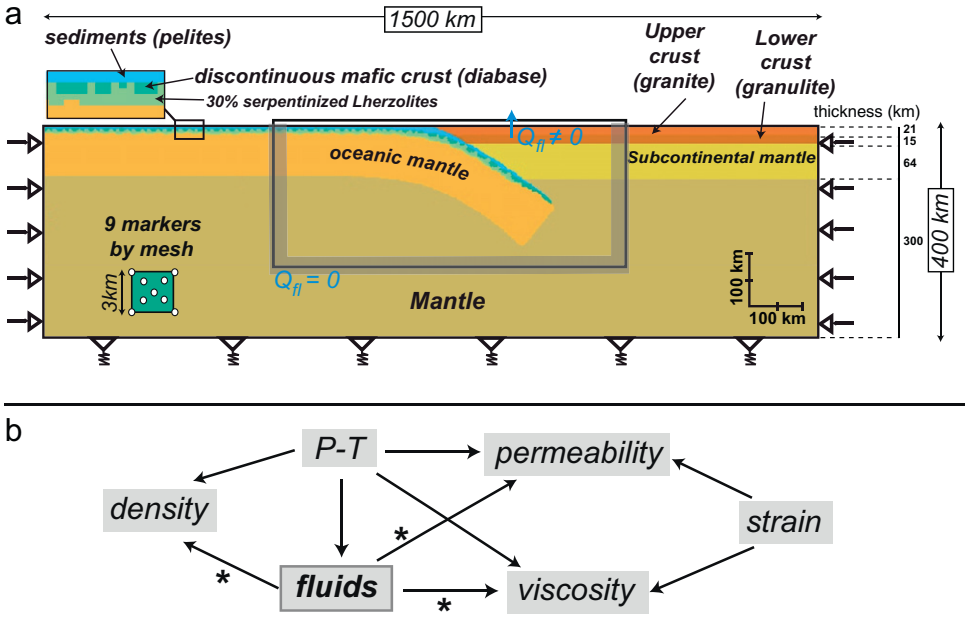

Fig. 2. (a) Initial setup for our oceanic subduction models with a close-up showing the detailed structure of the oceanic lithosphere (see Yamato et al., 2007 for further information on the setup). The fluid flow is computed only in the rectangle surrounding the subduction zone (see Appendix B in supplementary material for details). The amount of fluid is set to zero on the boundary of this box ($Q_{fl}=0$) except at the surface where the total fluid flux outwards the mesh elements is cancelled ($Q_{fl} \neq 0$) (that is, the quadrangles at the top of the mesh are not allowed to retain any fluid). (b) Sketch showing the complex interplays between all the variables considered in this study. *, relationship considered only for ultramafic material (serpentinites and peridotites).

conditions using thermodynamic free-energy minimisation (Connolly, 2005; Yamato et al., 2007).

2.2. Fluid circulation model

Given that metamorphic rocks porosity is extremely low, we considered as a first approximation that the instantaneous total water content equals the mineral-bounded water content. As an example, an element of the model made of serpentinite is considered to carry 12 wt.% H_2O. In our model, the instantaneous fluid content (which for instance may vary with prograde metamorphic dehydration reactions) is automatically derived from P–T-[H_2O] grids calculated with PerpleX (Connolly, 2005; Fig. 2b).

Although previous numerical models considered that fluids released by metamorphic reactions dominantly migrate upwards by porous flow along the vertical pressure gradient (e.g. Iwamori, 1998; Arcay et al., 2005), an increasing number of recent studies evoke the possibility that fluids do not necessarily migrate purely upwards but could also flow downwards or trenchwards (Hacker et al., 2003; Faccenda et al., 2009; Faccenda and Mancktelow, 2010; Kawano et al., 2011; van Keken et al., 2011). In order to better reproduce the complex coupling between deformation and fluid flow at depth in subduction zones, we formulated an alternative algorithm enabling released free fluids to migrate along the non-lithostatic pressure gradients, i.e., without any prescribed condition on the flow direction (e.g. Connolly and Podladchikov, 2004; Faccenda and Mancktelow, 2010). Fluid pressure in each element of the model is therefore proportional to non-lithostatic pressure (Appendix B in supplementary material) and the expelled fluid is forced to migrate from higher to lower non-lithostatic pressure domains (i.e., where deformation generally concentrates). The idea that these tectonic pressure gradients play a more important role than the vertical pressure gradient is supported by the fact that (i) pore connectivity is extremely low in metamorphic rocks (free fluids pressure therefore approaches lithostatic values; Etheridge et al., 1983; Connolly, 1997) and (ii) fractures, faults and shear zones constitute higher-permeability drains for fluids in natural systems (e.g. Cox, 2001; Ague, 2003; Miller et al., 2003; Angiboust et al., 2011).

In our model, fluid circulation also depends on the relative water saturation of the material (that is, in domains where non-lithostatic pressure is roughly constant, water flows from hydrated to anhydrous material; Appendix B in supplementary material). We also defined a “dynamic permeability” parameter, which itself depends on the strain rate (that is, fluid flow will be channelised within domains undergoing active deformation) and on P–T conditions (following the permeability-depth relationship of Ingebritsen and Manning, 1999). Introduction of a deformation-dependant permeability term enables considering the strong effect of an anisotropic fabric (that develop within rocks undergoing deformation) on fluid channelization (e.g. Kawano et al., 2011). This new algorithm was designed (i) to reproduce large-scale fluid circulation processes in order to take into account serpentinization processes (e.g. as in Gerya et al., 2002; Arcay et al., 2005; Iyer et al., 2010), (ii) to allow for a feedback between fluid content and mantle viscosities, densities and permeabilities (Fig. 2b). Detailed equations, constitutive relations and references are presented in Appendix B in supplementary material.

The fluid circulation starts after 2.5 Myr of convergence in order to first achieve a thermally and mechanically stable subduction environment (Yamato et al., 2007). While sediments are initially water-saturated, the oceanic mantle and the oceanic crust are considered to be initially moderately hydrated (~30% serpentinization; Ranero et al., 2003, and 2 wt.% H_2O, respectively; Carlson, 2003; Table 1). Note that the use of P–T-[H_2O] grids derived from pseudosection modelling implies that we assume that thermodynamic equilibrium is reached for each element of the model. Since our numerical experiments primarily aim at understanding the main parameters controlling the formation of large mafic slices in a serpentinized environment along the plate interface in relatively

Table 1
Chemical and rheological parameters used in the experiments.

Phase	Chemical composition (ox. wt.%)	Material	Reference	Initial water amount (wt.%)	Flow law reference	Experimental material	Viscosity parameters $\log_{10}(A)$ ($MPa^{-n} s^{-1}$)	n	Q (kJ mol^{-1})
Sediments	Si(50)Al(11.2)Fe(9.5)Mg(4.9)K(4)	Fe–Mg rich pelite	Yamato et al. (2007)	Saturated	Shea and Kronenberg (1992)	Micaschist	−67	31	98
					Ranalli and Murphy (1987)	Wet quartzite	−5.16	3	156
Serpentinite	Si(42.5)Al(1)Fe(6)Mg(42) Ca(1.5)	Serpentinized lherzolite	Li et al. (2004)[a]	4%	Hilairet et al. (2007)	Serpentinite	−12.6	5.8	18
Oceanic mafic crust	Si(49.8)Al(16.3)Fe(10.6)Mg(6.7)Ca(10.9)Na(3.1)	Basalt	Carmichael (1989)	2%	Caristan (1980)	Maryland diabase	−1.2	3.1	276
Upper continental crust	Si(70.2)Al(14.1)Fe(3.6)Mg(0.2)Ca(1.7)Na(3)K(6)	Granite	Carmichael (1989)	1%	Hansen and Carter (1983)	Wet westerly granite	−3.7	1.9	141
Lower continental crust	Si(50.1)Al(18.4)Fe(8.1)Mg(7.2)Ca(9.9)Na(3.4)	Mafic granulite	Forster et al. (2010)[a]	1%	Caristan (1980)	Maryland diabase	−1.2	3.1	276
Oceanic lithospheric mantle	Si(44.7)Al(3.9)Fe(8.2)Mg(36.7)Ca(3.2)	Abyssal peridotite	Workman and Hart (1995)	0%	Goetze and Evans (1979)	Dry olivine	3.84	3	510
Subcontinental mantle	Si(44)Al(2.3)Fe(8.4)Mg(41.4)Ca(2.15)	Spinel peridotite	McDonough (1990)	0%	Karato and Jung (2003)	Wet olivine	2.9	3	470
Mantle	Si(45)Al(4.5)Fe(8.1)Mg(37.8) Ca(3.6)	Primitive mantle	McDonough and Sun (1995)	0%	Goetze and Evans (1979)	Dry olivine	3.84	3	510

[a] Averaged chemical composition; Elastic parameters, cohesion, friction angle, thermal conductivity and diffusivity are identical to Yamato et al. (2007).

"cold" subduction zone settings, partial melting processes were ignored. In addition, phase relationships, melt formation and extraction processes are still debated (e.g. Poli and Schmidt, 2002) and have so far yielded contrasting numerical models (Hebert et al., 2009; Gerya and Meilick, 2011 and references therein).

3. Experiments and results

The following parameters were systematically varied in a series of experiments (summarised in Table 2): (i) the presence of fluid circulation, (ii) the structure of oceanic crust, (iii) the rheology of both the oceanic crust and sediments and (iv) the convergence rate. The best match with the behaviour inferred from field observations in the Western Alps was achieved in experiment Sub45, hereafter referred to as the reference experiment.

3.1. Reference experiment (sub45)

The results of this numerical experiment after 16.5 Myr of convergence are presented in the compositional map of Fig. 3a and in Table 2 (see Appendix C in supplementary material for the associated thermal structure, density, and strain rate maps). The oceanic lithosphere is buried along a rather cold gradient (~7°/km) in agreement with the prograde *P–T* path reported for the *W*. Alps ophiolitic domains (Agard et al., 2001; Angiboust et al., 2012b; Fig. 3b). We observe large pluri-kilometric fragments of oceanic crust, decoupled from the downgoing slab and accreted along the plate interface (Fig. 3a). Discontinuities within the oceanic crust (initially separated by serpentinized mantle directly overlain by sediments; Fig. 2a) are activated as thrusts during the detachment of these slices. Note that this slicing systematically occurs along pre-existing weakness zones, preserving a relatively undisturbed lateral continuity within individualised tectonic bodies. Importantly, these slices undergo very limited upwards motion but rather remain stacked along the plate interface, decoupled from the downgoing plate.

These fragments are underlain by a relatively thick (10–20 km) and buoyant, partly serpentinized sole (20–25% serpentinization; Fig. 4c). Sediments, which are the dominant material at shallow depths (0–40 km) along the subduction interface, are restricted to a narrow strip at mantle depths. The overlying mantle wedge appears stagnant under the continental Moho but is dragged beyond depths of 150 km together with the downgoing plate (Fig. 3a). After 16.5 Myr of convergence, most of the sedimentary material is scraped off and accreted within the accretionary wedge by underplating (as in Yamato et al., 2007; Plunder et al., 2012). At this stage, our model shows that the subduction channel is composed of 15% sediments, 31% mafics and 54% serpentinite between 60 and 100 km depth (i.e., typical depths exposed in the Western Alps internal high-pressure domain; Guillot et al., 2004; Angiboust and Agard, 2010; Table 2).

The dynamic permeability map (Fig. 3b; Appendix B in supplementary material) suggests the existence of 10–100 times higher permeability zones located below and at the top of the oceanic crust. Fluids produced by dehydration metamorphic reactions will therefore be drained along these "channels" where deformation is localised. The highest water contents (up to 6 wt.%) are reached in the accretionary wedge (Fig. 4a), where sedimentary material is close to saturation (Fig. 4b). The water content, originally comprised between 2 and 6 wt.% within the subducting lithosphere, decreases at the tip of the wedge to reach 2–3% on average (Fig. 4a). Note that even if the rocks are located at *P–T* conditions where major water release occurs (40–70 km depth), they remain undersaturated (Fig. 4b; i.e., water content is 2–3 times lower than theoretical maximum water contents,

Table 2
Summary of the numerical experiments, compared with the reference model (Sub45). Parameters changed with respect to Sub45 are highlighted by gray boxes. Sign "+" means presence.

Parametric study	**Parameter tested**				**Results**				
					Oceanic crust rheology				
	Plate velocity (cm yr^{-1})	**Fluid circulation**	**Serp. sole**	**Oceanic crust structure**	**Mafic crust**	**Sediments**	**Stability of subduction**	**Detachment of crustal fragments at 60–100 km depth and timing**	**Prop. of subd. channel crustal material at 60–100 km depth at 16 Ma**
Sub45 (ref. experiment)	2	+	+	Disc.	Maryland diabase	Micaschist	Stable	Large mafic fragments at ~10 Ma	$Sed_{15}Mafic_{31}Serp_{54}$
Sub45nofl	2			Disc.	Maryland diabase	Micaschist	Stable	No detachment	$Sed_{40}Mafic_{26}Serp_{34}$
Sub46	2	+		Disc.	Maryland diabase	Micaschist	Stable	No detachment	$Sed_{25}Mafic_{75}$
Sub46nofl	2			Disc.	Maryland diabase	Micaschist	Stable	No detachment	$Sed_{63}Mafic_{37}$
Sub48	2	+	+	Cont.	Maryland diabase	Micaschist	Stable	No detachment	$Sed_{24}Mafic_{45}Serp_{31}$
Sub43	2	+	+	Disc.	Maryland diabase	Wet quartzite	Slab breakdown at 13 Ma	Sedimentary "plume" in the mantle wedge at ~9.5 Ma	$Sed_{22}Mafic_{33}Serp_{45}$
Sub43nofl	2		+	Disc.	Maryland diabase	Wet quartzite	Stable	Accretion of sediments along the plate interface	$Sed_{65}Mafic_{22}Serp_{13}$
Sub43bis	2	+	+	Disc.	Wet quartzite	Wet quartzite	Slab breakdown at 10 Ma	Medium-sized fragments in a mélange at 6.6 Ma	No crust
Sub49	1	+	+	Disc.	Maryland diabase	Micaschist	Stable	Medium-sized slices at ~13 Ma	$Sed_{34}Mafic_{30}Serp_{36}$
Sub50	4	+	+	Disc.	Maryland diabase	Micaschist	Slab breakdown at 12 Ma	Medium-sized slices at ~10 Ma	$Sed_{25}Mafic_{45}Serp_{30}$
								Western Alps HP ophiolites proportions:	$Sed_{8}Mafic_{44}Serp_{48}$

assuming thermodynamic equilibrium). At greater depths (>100 km), water contents become very low (<1 wt.%), but the three orders of magnitude lower dynamic permeabilities prevent fluid draining, which explains the presence of oversaturated domains along and below the subduction interface down to ca. 300 km (Fig. 4b).

In order to better understand the extent of fluid infiltration within the mantle surrounding the subducted crust, we calculated the degree of serpentinization (i.e., the instantaneous water content divided by 12%, which is the amount of water within fully serpentinized peridotite; Fig. 4c). Maximum water contents calculated in the reference model suggest that a serpentinite-rich, fully hydrated mantle can theoretically be preserved down to ~90 km depth within the subducting slab (Fig. 3c). They also indicate that the upper mantle wedge, immediately below the continental Moho (40–50 km), may be fully hydrated (with 12 wt.% H_2O) for such a thermal regime of the subduction zone (Fig. 3c). A narrower (10–15 km thick) front located at the top of the subduction interface also develops down to 150 km depth (where Mg-chlorite breaks down at ca. 800 °C; Fig. 3b) and exhibits slightly lower serpentinization degree, on the order of 5–15% (Fig. 4c). The extent of initial serpentinization of the oceanic mantle (around 35% prior to subduction) progressively decreases to reach ~15–20% at 100 km depth (Fig. 4c). As expected, slab bending produces intensive normal faulting in the hinge area (Ranero et al., 2003; Faccenda et al., 2012), thereby increasing mantle permeability and permitting fluid infiltration down to ca. 30 km depth within the mantle (Figs. 3 and 4; Appendix C in supplementary material).

3.2. Parametric study

In order to first evaluate the mechanical impact of fluids on subduction interface dynamics, the fluid circulation algorithm was turned off in experiment sub45nofl, keeping all other parameters as in the reference model. Results (Table 2) show that in absence of fluid circulation, no fragments of oceanic crust are ever detached from the downgoing slab during the experiment (20 Myr). A larger sedimentary component is also observed along the plate interface (40% sediments instead of 15% in the reference model).

In order to evaluate the influence of an initial serpentinite sole (as expected from seafloor serpentinization of the oceanic mantle; e.g. Iyer et al., 2010), another experiment was performed in which the discontinuous oceanic crust directly lies on the dry oceanic mantle (sub46). This configuration yields results similar to the previous experiment and does not lead to the detachment of oceanic crust fragments, whether or not activating the fluid circulation algorithm (sub46nofl; Fig. 5a). Note that the subduction of an initially continuous oceanic crust (sub48) also prevents the slice detachment observed in the reference experiment (cf. Table 2).

The use of different rheological flow laws is known to be a major source of discrepancies between numerical models (e.g. Kaus et al., 2009). Evaluating the effect of sediment rheology is therefore of critical importance for the modelling of subduction processes because their properties partly control the mechanical strength of the plate interface. While a micaschist flow law was used for the reference experiment (Shea and Kronenberg, 1992), an alternative wet quartzite flow law, substantially weaker (viscosity is 1.3 order of magnitude lower at 500 °C) and commonly used in geodynamic numerical modelling (e.g. Currie et al., 2007; Yamato et al., 2007; Warren et al., 2008; Gerya and Meilick, 2011), was used in exp. Sub43 (Table 2; Fig. 5b). We observe the formation of a buoyant sedimentary "plume" (similar to those first described by Gerya and Yuen, 2003) after 4 Myr of

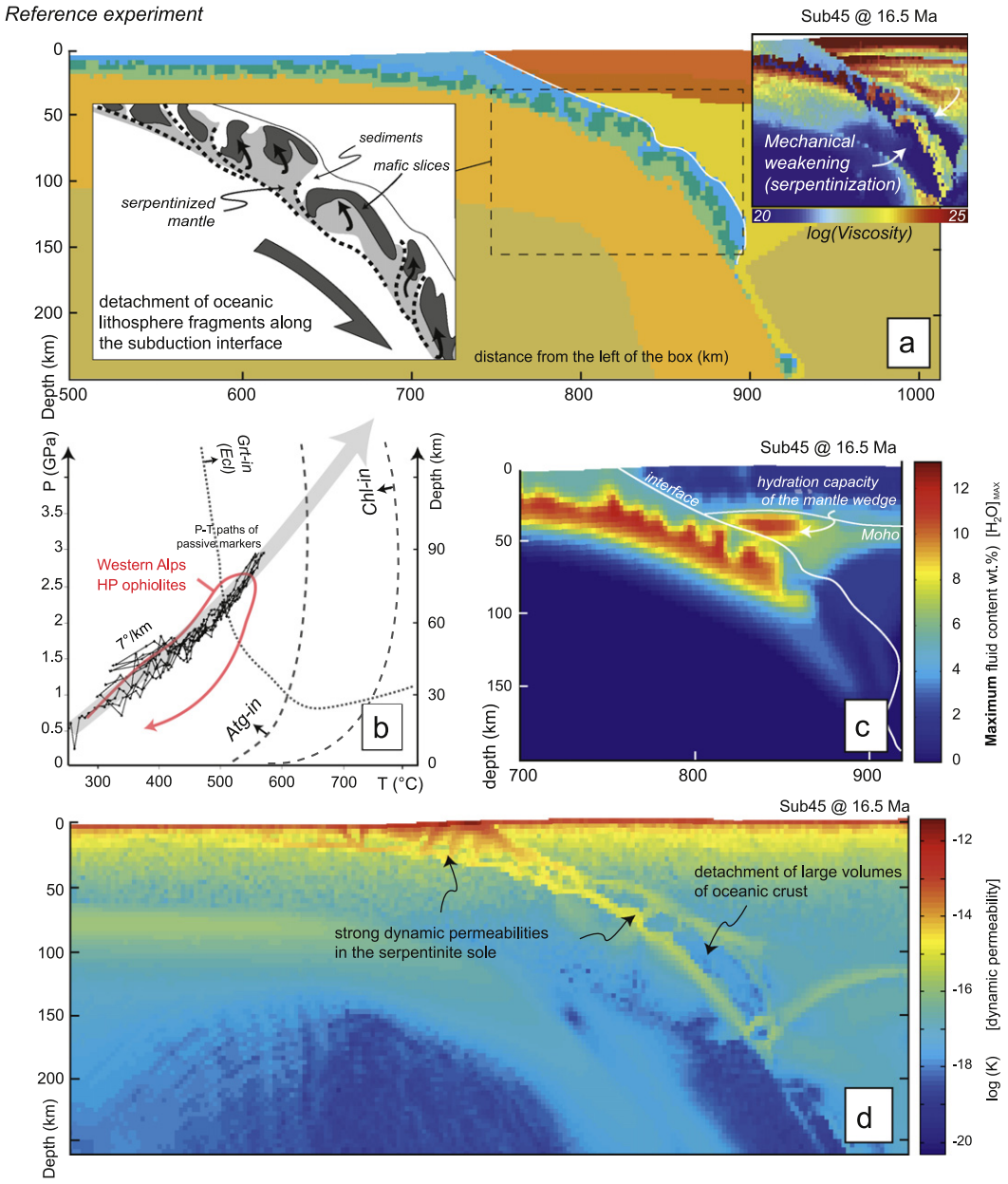

Fig. 3. (a) Morphology of our reference experiment (Sub45) after 16.5 Myr of convergence (i.e., the time step at which tectonic slices were the most obvious during model evolution). The inset shows the distribution of effective viscosity within the subduction zone for the same time-step. (b) Burial *P–T* paths obtained for downgoing oceanic lithosphere showing excellent agreement with prograde *P–T* paths from the literature for eclogite-facies Alpine ophiolitic units (see references in the text). Also shown three major water-producing phase transitions associated with eclogitization of the oceanic crust and the breakdown of antigorite and chlorite within ultramafics. (c) Close-up view showing the maximum fluid content (in wt.% H_2O) theoretically permitted, computed for each element of the mesh (based on thermodynamic data using the program PerpleX). (d) "Dynamic permeability" structure of the reference experiment after 16.5 Myr of convergence showing the presence of higher-permeability channels forming in deforming areas (with higher strain rates; Appendix C in supplementary material), surrounding lower-permeability domains (decoupled oceanic crust).

convergence. This low-viscosity, buoyant instability develops within the hydrated mantle wedge (Hebert et al., 2009) and progressively reaches the continental Moho. In this case a break-off of the downgoing slab takes place at ca. 13 Myr. Note that the same experiment run without fluid circulation (sub43-nofl) produces a very thick accretionary wedge along the subduction interface down to ca.90 km depth, probably in response to changes in interplate mechanical coupling.

We also tested the effect of the presence of a very weak mafic oceanic crust by using a wet quartzite flow law instead of the diabase rheology (Gerya and Meilick, 2011; sub43bis; Table 2; Fig. 5c). An accretionary complex (similar to the one formed in experiment sub43nofl) formed after 6 Myr of convergence, showing a very complex tectonic mixing between the oceanic lithosphere fragments and the mantle wedge. Weakening of the oceanic crust thus does not promote the detachment of large tectonic slices along the subduction interface between 60 and 100 km depth but apparently rather favours the formation of various types of sediment-rich accretionary complexes and/or plume-like sedimentary instabilities.

Finally, only minor changes with respect to the reference experiment are observed when dividing the convergence rate by two (Sub49): these are (i) a higher sediment fraction along the subduction interface and (ii) the detachment of slightly smaller tectonic slices (Table 2). On the contrary, doubling the convergence rate (up to 4 cm yr^{-1}; Sub50) causes a break-off of the oceanic lithosphere at 12 Myr, following the detachment of similar medium-sized tectonic slices along the plate interface.

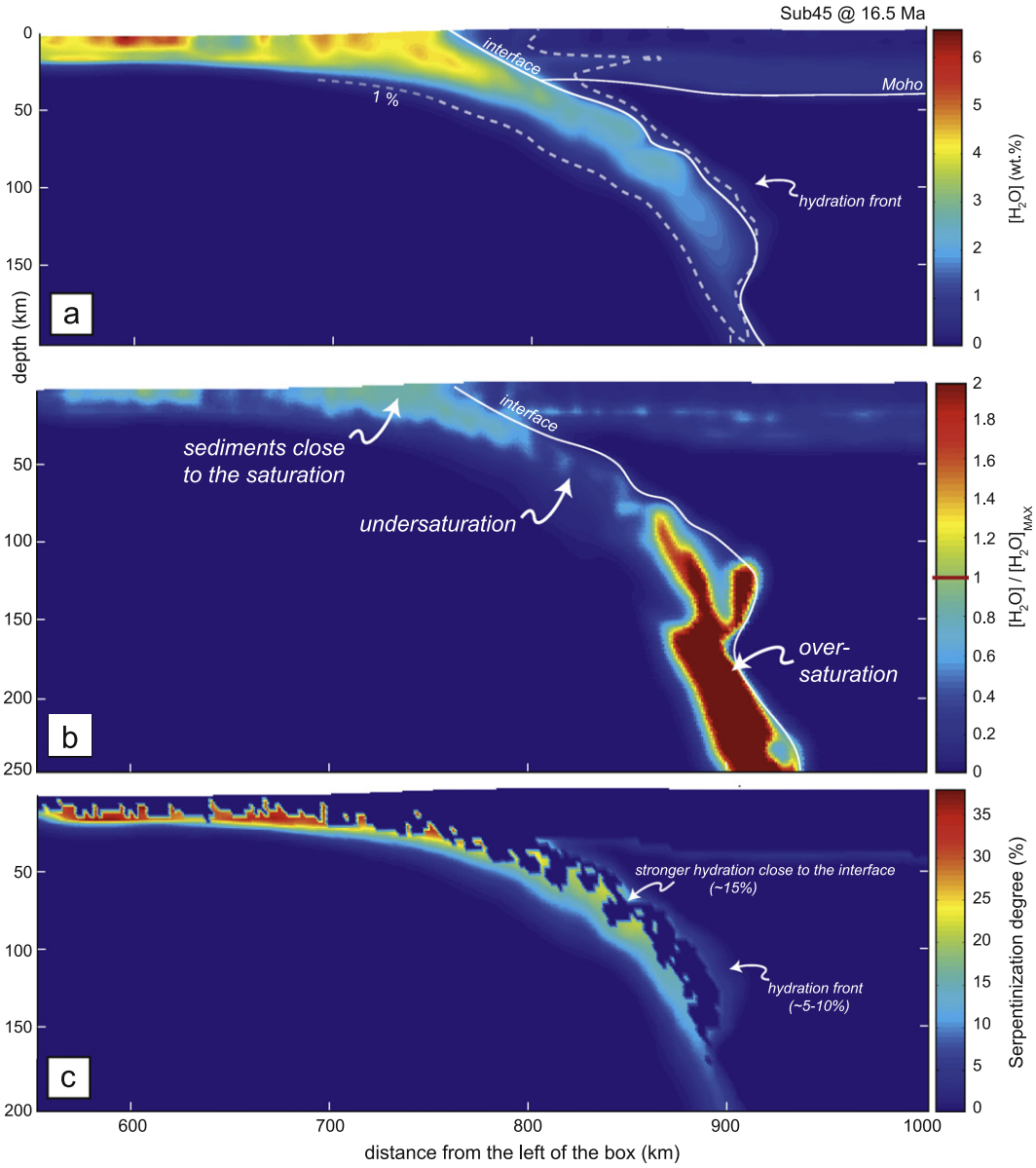

Fig. 4. (a) Water content of the reference experiment after 16.5 Myr of convergence showing a water-enriched accretionary wedge and decreasing water content with increasing depth. (b) Saturation ratio (obtained by normalising instantaneous water content by the maximum water content thermodynamically permitted for each material) for the reference experiment showing strong along-strike variations. Note that "over-saturated" domains exist at depth (100–250 km) below the subduction interface, where permeability is too low for fluid expulsion. (c) Serpentinization degree (calculated by dividing the instantaneous amount of fluid by 12 wt.%, i.e., the maximum weight amount of water within serpentinite) for the reference experiment at 16.5 Myr illustrating (i) the decrease of the serpentinization degree of oceanic peridotites with burial and (ii) the formation of a weak, diffuse hydration front close to the subduction interface at mantle depths.

4. Implications for subduction interface processes

These results throw light on the nature of the subduction interface and potentially help interpreting geophysical observations on active subduction zones. Comparing these results with field evidence from exhumed ophiolitic terrains also provides new insights on interplate petrological and tectonic processes acting in the mantle depth interval between 50 and 150 km.

4.1. Fluids: a key parameter controlling the formation of large oceanic lithosphere slices

Our experiments show that large pluri-kilometric volumes of oceanic lithosphere can be accreted between 50 and 110 km along the subduction interface. Although buoyancy is commonly regarded as a critical parameter permitting the exhumation and preservation of HP ophiolitic domains (Hermann et al., 2000; Schwartz et al., 2001; Yamato et al., 2007), our results suggest that this condition alone is not sufficient to enable slicing of the oceanic crust in the subduction channel (in line with Angiboust and Agard, 2010). The detachment of the sliced fragments is herein controlled by the interplay between buoyancy forces and the significant mechanical weakening resulting from the serpentinization of the subduction interface (mantle viscosity decreases by one to two orders of magnitude, in agreement with Billen and Gurnis, 2001; Hilairet et al., 2007; Appendix C in supplementary material; Table 2). These experiments also indicate that the existence of an initially discontinuous mafic crust facilitates the "basal decoupling" responsible for the detachment of these slices. We consequently hypothesise that slow-spreading oceans may be more subject to slice individualisation and detachment than those with a thick, continuous oceanic crust.

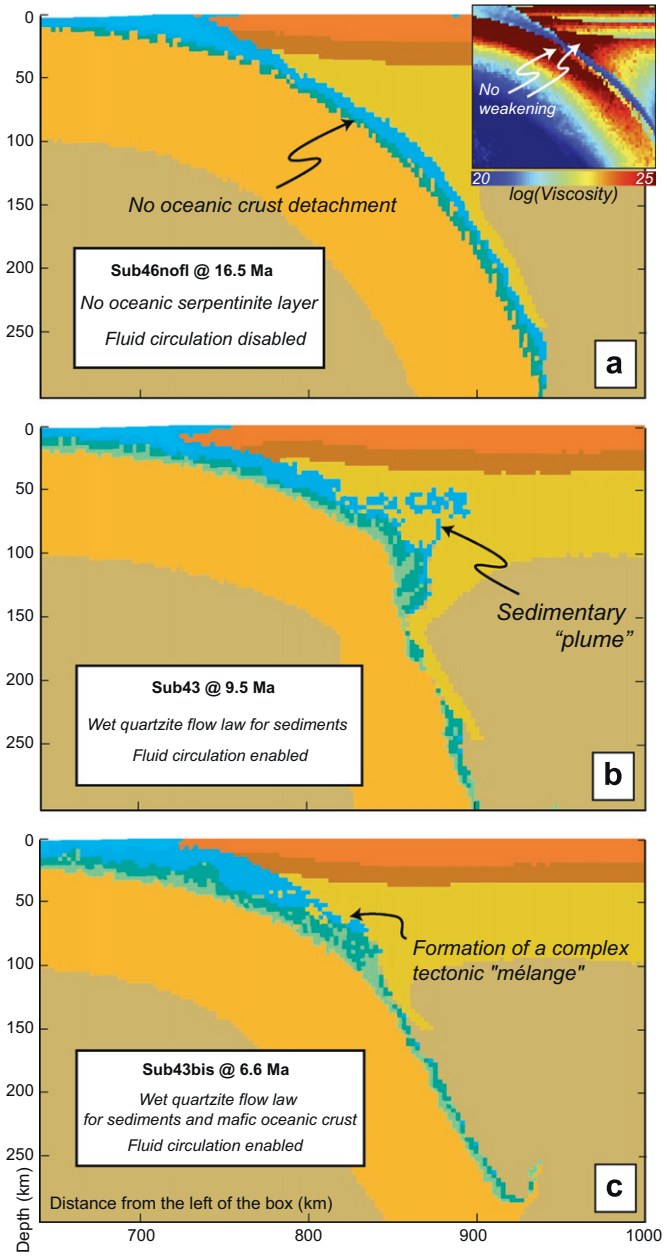

Fig. 5. (a) Morphology of the experiment Sub46nofl after 16.5 Myr of convergence showing the absence of detachment of large oceanic crust fragments. The inset shows the effective viscosity distribution for the same time-step in the absence of fluids. (b) Morphology of the experiment Sub43 after 9.5 Myr of convergence showing the formation of a "sedimentary plume" in the mantle wedge. (c) Morphology of the experiment Sub43bis after 6.6 Myr of convergence showing the formation of a complex tectonic mélange along the subduction interface where mantle wedge peridotites, oceanic crust and oceanic serpentinites are chaotically gathered.

Internal high-pressure ophiolitic massifs from the W. Alps or Alpine Corsica, exhumed from ca. 80 km depth (Angiboust et al., 2009; Vitale-Brovarone et al., 2011), indeed generally exhibit a striking primary first-order structural coherency, characterised by the presence of a relatively thick (~1 km) serpentinized oceanic mantle sole at the bottom of the ophiolitic pile (Angiboust and Agard, 2010). This suggests that a basal decoupling, taking place below the oceanic Moho, possibly at the transition between highly and weakly serpentinized peridotites, controlled the detachment of these slices. Note that the existence of reversed polarity km-sized ophiolitic tectonic slices in the Alpine orogen (e.g. Monviso Unit, Lombardo et al., 1978; Angiboust et al., 2012b) supports the possibility that kilometre-scale dragging folds formed during the detachment of the slice or on exhumation (Fig. 6).

The presence of such large slices in active subduction settings has been recently demonstrated by seismic data in the depth interval from 40 to 80 km beneath Tokyo (Toda et al., 2008). Our results suggest that such slab fragments may detach in subduction zones in response to a strong hydration of the oceanic lithosphere and/or in association with the scrapping off of downgoing asperities (such as seamounts; Ranero and Von Huene, 2000; Wang and Bilek, 2011) and/or mega-earthquakes (Singh et al., 2011). Although the subduction interface in the depth range 50–110 km is the source area of these tectonic slices in our models, we stress that (i) these slices underwent very limited upwards motion (few kilometres at the most) and that (ii) none of these slices escaped the subduction channel to reach the tip of the accretionary wedge (i.e., above ca. 35 km). Despite the fact that such a slicing of the oceanic lithosphere may be a long-lived process in active subduction zones, we indeed recall that the exhumation of HP rocks is only a transient process likely taking place during geodynamic perturbations of the subduction regime (Agard et al., 2007, 2009; Brun and Faccenna, 2008; Guillot et al., 2009). In the Western Alps, the exhumation and preservation of large volumes of eclogitized oceanic lithosphere were probably enabled by the entrance and rapid exhumation of buoyant continental material (i.e., internal crystalline massifs such as Dora Maira, Monte Rosa) plucking back the ophiolitic nappe-stack out of the subduction channel (e.g. Angiboust and Agard, 2010).

4.2. Constraints on subduction channel rheology

Fluids generated by prograde metamorphic dehydration reactions are channelised in our models in weaker materials (i.e., sediments and serpentinites), where deformation concentrates, and deflected around fragments of stronger, less permeable oceanic crust (Fig. 6). Subduction-parallel upwards fluid flux apparently dominates over subduction-perpendicular fluid infiltration, in close agreement with recent experimental studies on serpentinite permeability anisotropy (Kawano et al., 2011).

Our results suggest that the overlying mantle wedge only undergoes a slight serpentinization (10–15%) restricted to the vicinity of the plate interface (generally ~10 km-thick). These values, predicted for an Alpine-type subduction setting, are in agreement with geophysical studies suggesting the existence of a narrow, heterogeneous, slightly serpentinized mantle wedge in relatively "cold" subduction settings (~20%; Hyndman and Peacock, 2003; Chou et al., 2009). Note that in the reference experiment, material from the overlying mantle wedge is not dragged within the subduction channel, in line with geochemical data suggesting that serpentinized peridotites from the Western Alps effectively belong to the exhumed oceanic mantle (e.g. Hattori and Guillot, 2007). Interestingly, our models showed that dragging of mantle wedge material within the subduction channel occurs dominantly when the downgoing oceanic crust is modelled using weaker lithologies (Fig. 5c) and when the overriding mantle wedge is partly serpentinized.

The oceanic mantle also undergoes a slightly stronger downward serpentinization (10–20%) down to 20–30 km, in agreement with recent models suggesting that plate bending favours downward fluid flow inside the slab (Faccenda and Mancktelow, 2010). This deeper infiltration may potentially trigger seismic activity due to elevated pore fluid pressures (Fig. 4c), which in turn may explain the lower seismic plane frequently observed within active subduction zones (e.g. Hacker et al., 2003; Faccenda et al., 2012; Figs. 1 and 6). Our models do not permit to discriminate

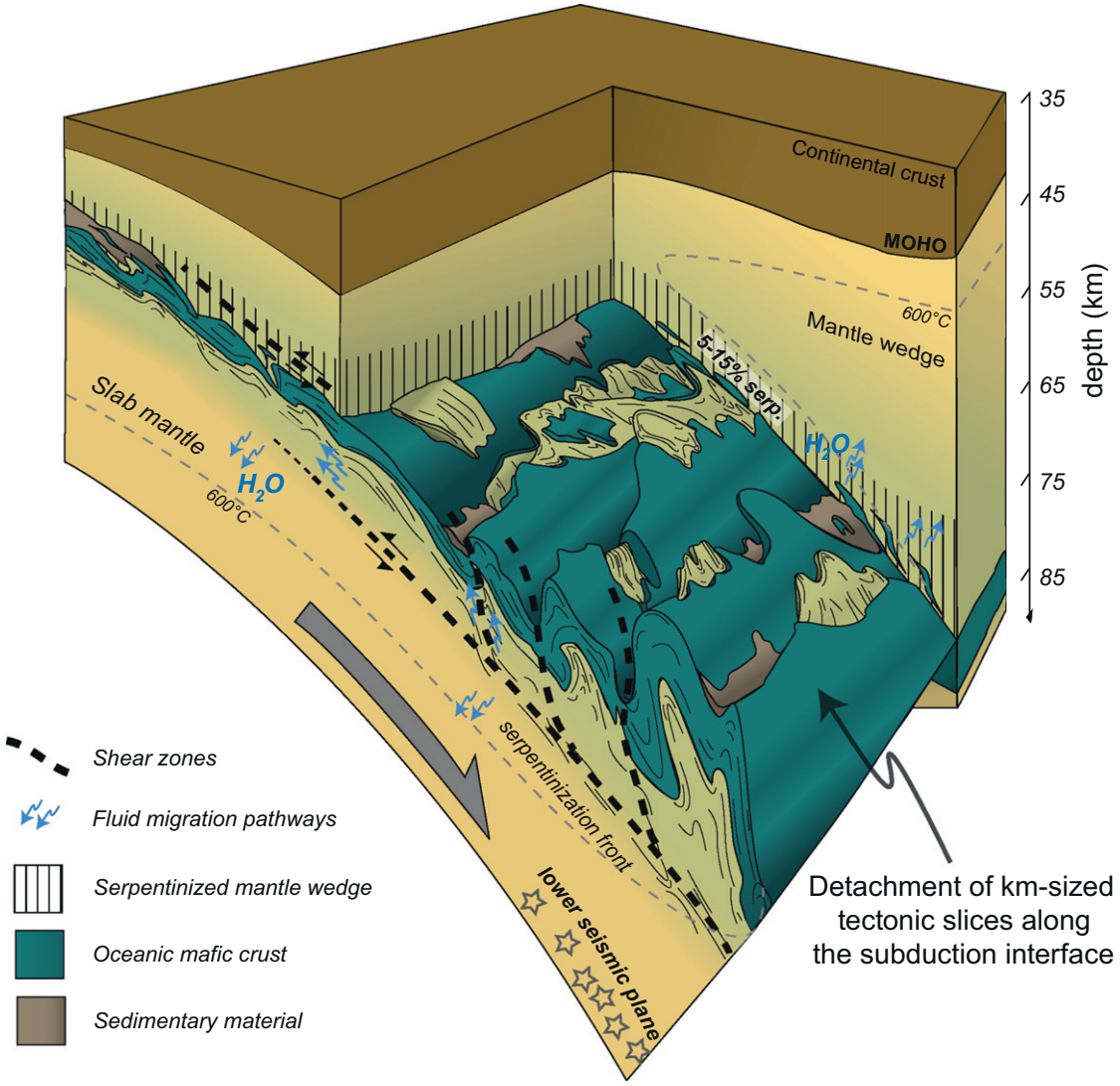

Fig. 6. Schematic view of a subduction zone between 35 and 85 km depth based on our numerical model results (and to a lesser extent on exhumed ophiolitic terrains) showing inferred morphologies and the detachment of large folded slices of oceanic lithosphere, accreted along the plate interface. This figure also illustrates the main deformation-enhanced fluid pathways (associated with deep serpentinite producing/consuming reactions), dominantly at the boundary between material with marked rheological contrasts.

accurately the origin of the upper plane seismicity (hydraulic fracturing and/or dehydration embrittlement; Davies, 1999; Hacker et al., 2003). The formation of a slightly serpentinized layer on the top of the subduction interface is generally believed to inhibit the formation of subduction thrust earthquakes (e.g. Hirauchi et al., 2010) because shear stress would be preferentially accommodated by plastic flow. Our results nevertheless show that pre-subduction segmentation of the oceanic lithosphere controls the formation of tectonic slices by reactivating inherited structural features (see also Butler, 1989). The latter could potentially cause intra-slab seismic events, as recorded within fossil and active subduction zones (Oncken et al., 1999; Rietbrock and Waldhauser, 2004; Marot et al., 2012; Angiboust et al., 2012a).

We finally stress that natural data (structure and lithological composition) from the W. Alps ophiolitic belt was better reproduced using relatively stronger rheologies for the oceanic crust (see Table 2). The choice of weaker rheologies for the sediments and mafic crust not only increases the thickness of the channel (and the relative fraction of sediments), but also influences the deformation style by promoting the formation of an accretionary complex (Fig. 5c) in which chaotic mixing and plume-like instabilities may develop (i.e., one of the characteristic features reported for several ophiolitic suture zones such as in Cuba or in the Franciscan complex; Cloos, 1982; Blanco-Quintero et al., 2011; Gerya and Meilick, 2011).

5. Conclusions

Thermo-mechanically and thermodynamically coupled numerical experiments accounting for fluid circulation enable a new understanding of the complex interplay between fluid and deformation at mantle depths within subduction zones. These experiments notably provide constraints on interplate mechanical coupling and on processes responsible for the detachment of oceanic lithosphere fragments.

Our results provide constraints on the rheology of the subduction interface between 50 and 150 km depth and suggest that the exhumation style within subduction zones (i.e., large tectonics slices versus complex mélanges) is partly controlled by the strength of subducted crustal material. In particular, we showed that a weak downgoing oceanic crust apparently promotes the formation of large mélange-like accretionary complexes while

large tectonic slices rather require a stronger, discontinuous oceanic crust overlying a serpentinized mantle.

These results (i) corroborate field evidence from large eclogitized tectonic slices of ophiolitic material showing homogeneous *P–T* conditions (i.e., tens of kilometres along-strike, as in the Western Alps) and (ii) are strongly supported by recent geophysical studies imaging the presence of decoupled oceanic material fragments in active subduction zones. We thus hypothesise that the detachment of such slices from the subducting plate represents a fraction of the intermediate-depth seismicity presently recorded within active subduction zones.

Acknowledgements

We thank Laetitia Le Pourhiet, Peter Van Keken, Benjamin Huet and Thomas François for insightful discussions and technical assistance. This paper benefited from thoughtful and careful reviews from Taras Gerya and Clare Warren.

Appendix A. Supporting information

Supplementary data associated with this article can be found in the online version at http://dx.doi.org/10.1016/j.epsl.2012.09.012.

References

Abers, G.A., 2005. Seismic low-velocity layer at the top of subducting slabs: observations, predictions, and systematics. Phys. Earth Planet. Inter. 149, 7–29.
Agard, P., Jolivet, L., Goffé, B., 2001. The Schistes lustrés complex: a key for understanding the exhumation of HP and UHP rocks in the Western Alps? Bull. Soc. Geol. Fr. 172, 617–636.
Agard, P., Jolivet, L., Vrielynck, B., Burov, E., Monié, P., 2007. Plate acceleration: the obduction trigger? Earth Planet. Sci. Lett. 258, 428–441.
Agard, P., Yamato, P., Jolivet, L., Burov, E., 2009. Exhumation of oceanic blueschists and eclogites in subduction zones: timing and mechanisms. Earth Sci. Rev. 92, 53–79.
Ague, 2003. Fluid flow in the deep crust. In: Rudnick, R.L. (Ed.), Treatise in Geochemistry. Elsevier.
Angiboust, S., Agard, P., Yamato, P., Raimbourg, H., 2012a. Eclogite breccias in a subducted ophiolite: a record of intermediate-depth earthquakes? Geology 40, 707–710.
Angiboust, S., Langdon, R., Agard, P., Waters, D., Chopin, C., 2012b. Eclogitization of the Monviso ophiolite and implications on subduction dynamics. J. Metamorph. Geol. 30, 37–61.
Angiboust, S., Agard, P., Raimbourg, H., Yamato, P., Huet, B., 2011. Subduction interface processes recorded by eclogite-facies shear zones. Lithos 127, 222–238.
Angiboust, S., Agard, P., 2010. Initial water budget: the key to detaching large volumes of eclogitized oceanic crust along the subduction channel? Lithos 120, 453–474.
Angiboust, S., Agard, P., Jolivet, L., Beyssac, O., 2009. The Zermatt-Saas ophiolite: the largest (60-km wide) and deepest (c. 70–80 km) continuous slice of oceanic lithosphere detached from a subduction zone? Terra Nova 21, 171–180.
Arcay, D., Tric, E., Doin, M.P., 2005. Numerical simulations of subduction zones: effect of slab dehydration on the mantle wedge dynamics. Phys. Earth Planet. Inter. 149, 133–153.
Audet, P., Bostock, M.G., Christensen, N.I., Peacock, S.M., 2009. Seismic evidence for overpressured subducted oceanic crust and megathrust fault sealing. Nature 457, 76–78.
Bachmann, R., Oncken, O., Glodny, J., Seifert, W., Georgieva, V., Sudo, M., 2009. Exposed plate interface in the European Alps reveals fabric styles and gradients related to an ancient seismogenic coupling zone. J. Geophys. Res. 114, B05402.
Billen, M.I., Gurnis, M., 2001. A low viscosity wedge in subduction zones. Earth Planet. Sci. Lett. 193, 227–236.
Blanco-Quintero, I.F., Garcia-Casco, A., Gerya, T.V., 2011. Tectonic blocks in serpentinite melange (eastern Cuba) reveal large-scale convective flow of the subduction channel. Geology 39, 79–82.
Brun, J.P., Faccenna, C., 2008. Exhumation of high-pressure rocks driven by slab rollback. Earth Planet. Sci. Lett. 272, 1–7.
Burov, E., Jolivet, L., Le Pourhiet, L., Poliakov, A., 2001. A thermomechanical model of exhumation of high pressure (HP) and ultra-high pressure (UHP) metamorphic rocks in Alpine-type collision belts. Tectonophysics 342, 113–136.
Burov, E.B., Diament, M., 1995. The effective elastic thickness (Te) of continental lithosphere: what does it really mean? J. Geophys. Res. 100 (B3), 3905–3927.
Butler, R.W.H., 1989. The Influence of Pre-existing Basin Structure on Thrust System Evolution in the Western Alps, 44. Geological Society, London (Special Publication), pp. 105–122.
Cannat, M., Lagabrielle, Y., Bougault, H., Casey, J., De Coutures, N., Dmitriev, L., Ultramafic and gabbroic exposures at the Mid-Atlantic ridge: geological mapping in the 15°N region. Tectonophysics 279, 197–213.
Caristan, Y., 1980. High Temperature Mechanical Behavior of Maryland Diabase. Ph.D. thesis, MIT, Cambridge, MA.
Carlson, R.L., 2003. Bound water content of the lower oceanic crust estimated from modal analyses and seismic velocities of oceanic diabase and gabbro. Geophys. Res. Lett. 30 (22), 2142.
Carmichael, R., 1989. Practical Handbook of Physical Properties of Rocks and Minerals. CRC Press, Boca Raton, FL 741 pp.
Chou, H.C., Kuo, B.Y., Chiao, L.Y., Zhao, D., Hung, S.H., 2009. Tomography of the westernmost Ryukyu subduction zone and the serpentinization of the fore-arc mantle. J. Geophys. Res. 114, B12301.
Cloos, M., 1982. Flow Melanges -– numerical modeling and geologic constraints on their origin in the franciscan subduction complex, California. Geol. Soc. Am. Bull. 93, 330–345.
Connolly, J.A.D., 2005. Computation of phase equilibria by linear programming: a tool for geodynamic modeling and its application to subduction zone decarbonation. Earth Planet. Sci. Lett. 236, 524–541.
Connolly, J.A.D., Podladchikov, Y.Y., 2004. Fluid flow in compressive tectonic settings: implications for midcrustal seismic reflectors and downward fluid migration. J. Geophys. Res. 109, B04201.
Connolly, J.A.D., 1997. Deformation-generated fluid pressure and deformation-propagated fluid flow during regional metamorphism. J. Geophys. Res. 102, 18149–18173.
Contreras-Reyes, E., Carrizo, D., 2011. Control of high oceanic features and subduction channel on earthquake ruptures along the Chile–Peru subduction zone. Phys. Earth Planet. Inter. 186, 49–58.
Cox, S.F., 2001. Fluid flow in mid- to deep crustal shear systems: experimental constraints, observation on exhumed high fluid flux shear systems, and implications on seismogenic processes. Earth Planets Space 54, 1121–1125.
Cundall, P.A., 1989. Numerical experiments on localization in frictional materials. Arch. App. Mech. 59, 148–159.
Currie, C.A., Beaumont, C., Huismans, R.S., 2007. The fate of subducted sediments: a case for backarc intrusion and underplating. Geology 35, 1111–1114.
Davies, J.H., 1999. The role of hydraulic fractures and intermediate-depth earthquakes in generating subduction-zone magmatism. Nature 398, 142–145.
Etheridge, M.A., Wall, V.J., Cox, S.F., 1983. High fluid pressures during regional metamorphism and deformation: implications for mass transport and deformation mechanism. J. Geophys. Res. 86, 4344–4358.
Faccenda, M., Gerya, T.V., Burlini, L., 2009. Deep slab hydration induced by bending-related variations in tectonic pressure. Nat. Geosci. 2, 790–793.
Faccenda, M., Gerya, T.V., Mancktelow, N.S., Moresi, L., 2012. Fluid flow during slab unbending and dehydration: implications for intermediate-depth seismicity, slab weakening and deep water recycling. Geochem. Geophys. Geosyst. 13, Q01010.
Faccenda, M., Mancktelow, N.S., 2010. Fluid flow during unbending: implications for slab hydration, intermediate-depth earthquakes and deep fluid subduction. Tectonophysics 494, 149–154.
Forster, H.J., Forster, A., Oberhansli, R., Stromeyer, D., 2010. Lithospheric composition and thermal structure of the Arabian Shield in Jordan. Tectonophysics 481, 29–37.
Gerya, T.V., Meilick, F.I., 2011. Geodynamic regimes of subduction under an active margin: effects of rheological weakening by fluids and melts. J. Metamorph. Geol. 29, 7–31.
Gerya, T.V., Stockhert, B., Perchuk, A.L., 2002. Exhumation of high-pressure metamorphic rocks in a subduction channel: a numerical simulation. Tectonics, 21.
Gerya, T.V., Yuen, D.A., 2003. Rayleigh-Taylor instabilities from hydration and melting properties of cold plumes at subduction zones. Earth Planet. Sci. Lett. 212, 47–62.
Goetze, C., Evans, B., 1979. Stress and temperature in the bending lithosphere as constrained by experimental rock mechanics. Geophys. J. R. Astron. Soc. 59, 463–478.
Gorczyk, W., Guillot, S., Gerya, T.V., Hattori, K., 2007. Asthenospheric upwelling, oceanic slab retreat, and exhumation of UHP mantle rocks: insights from Greater Antilles. Geophys. Res. Lett., 34.
Green, H.W., Houston, H., 1995. The mechanics of deep earthquakes. Ann. Rev. Earth Planet. Sci. 23, 169–213.
Green, H.W., Chen, W.P., Brudzinski, M.R., 2010. Seismic evidence of negligible water carried below 400-km depth in subducting lithosphere. Nature 467, 828–831.
Guillot, S., Schwartz, S., Hattori, K., Auzende, A., Lardeaux, J., 2004. The Monviso Ophiolitic Massif (Western Alps), A Section Through a Serpentinite Subduction Channel. Evolution of the Western Alps: Insights from Metamorphism, Structural Geology, Tectonics and Geochronology, The Virtual Explorer, Paper 3.
Guillot, S., Hattori, K., Agard, P., Schwartz, S., Vidal, O., 2009. Exhumation Processes in Oceanic and Continental Subduction Contexts: A Review, Subduction Zone Geodynamics. Frontiers in Earth Sciences. Springer Berlin Heidelberg, pp. 175–205.

Hacker, B.R., Peacock, S.M., Abers, G.A., Holloway, S.D., 2003. Subduction factory – 2. Are intermediate-depth earthquakes in subducting slabs linked to metamorphic dehydration reactions? J. Geophys. Res.-Solid Earth 108 (B1).
Hansen, F.D., Carter, N.L., 1983. Semibrittle Creep Of Dry And Wet Westerly Granite At 1000 MPa. Conference paper: The 24th U.S. Symposium on Rock Mechanics (USRMS), June 20–23, 1983. College Station, TX.
Hattori, K.H., Guillot, S., 2007. Geochemical character of serpentinites associated with high- to ultrahigh-pressure metamorphic rocks in the Alps, Cuba, and the Himalayas: recycling of elements in subduction zones. Geochem. Geophys. Geosyst. 8, Q09010.
Hebert, L.B., Antoshechkina, P., Asimow, P., Gurnis, M., 2009. Emergence of a low-viscosity channel in subduction zones through the coupling of mantle flow and thermodynamics. Earth Planet. Sci. Lett. 278, 243–256.
Hermann, J., Müntener, O., Scambelluri, M., 2000. The importance of serpentinite mylonites for subduction and exhumation of oceanic crust. Tectonophysics 327, 225–238.
Hilairet, N., et al., 2007. High-pressure creep of serpentine, interseismic deformation, and initiation of subduction. Science 318, 1910–1913.
Hilairet, N., Reynard, B., 2009. Stability and dynamics of serpentinite layer in subduction zone. Tectonophysics 465, 24–29.
Hirauchi, K.-i., Katayama, I., Uehara, S., Miyahara, M., Takai, Y., 2010. Inhibition of subduction thrust earthquakes by low-temperature plastic flow in serpentine. Earth Planet. Sci. Lett. 295, 349–357.
Hyndman, R.D., Peacock, S.M., 2003. Serpentinization of the forearc mantle. Earth Planet. Sci. Lett. 212, 417–432.
Ingebritsen, S.E., Manning, C.E., 1999. Geological implications of a permeability-depth curve for the 178 continental crust. Geology 27, 1107–1110.
Iwamori, H., 1998. Transportation of H_2O and melting in subduction zones. Earth Planet. Sci. Lett. 160, 65–80.
Iyer, K., Rüpke, L.H., Morgan, J.P., 2010. Feedbacks between mantle hydration and hydrothermal convection at ocean spreading centers. Earth Planet. Sci. Lett. 296, 34–44.
Jung, H., 2011, Seismic anisotropy produced by serpentine in mantle wedge. Earth Planet. Sci. Lett. 307, 535–543.
Karato, S.-i., Jung, H., 2003. Effects of pressure on high-temperature dislocation creep in olivine. Philos. Mag., 83.
Kaus, B.J.P., Liu, Y., Becker, T.W., Yuen, D.A., Shi, Y., 2009. Lithospheric stress-states predicted from long-term tectonic models: influence of rheology and possible application to Taiwan. J. Asian Earth Sci. 36, 119–134.
Kawano, S., Katayama, I., Okazaki, K., 2011. Permeability anisotropy of serpentinite and fluid pathways in a subduction zone. Geology 39, 939–942.
Kodaira, S., et al., 2004. High pore fluid pressure may cause silent slip in the Nankai Trough. Science 304, 1295–1298.
Kuge, K., Kase, Y., Urata, Y., Campos, J., Perez, A., 2010. Rupture characteristics of the 2005 Tarapaca, northern Chile, intermediate-depth earthquake: evidence for heterogeneous fluid distribution across the subducting oceanic plate? J. Geophys. Res. 115 (B9), B09305.
Lagabrielle, Y., Lemoine, M., 1997. Alpine, Corsican and Apennine ophiolites: the slow-spreading ridge model. C. R. Acad. Sci.–Ser. IIA – Earth Planet. Sci. 325, 909–920.
Lagabrielle, Y., Cannat, M., 1990. Alpine Jurassic ophiolites resemble the modern central Atlantic basement. Geology 18, 319–322.
Li, X.P., Rahn, M., Bucher, K., 2004. Serpentinites of the Zermatt-Saas ophiolite complex and their texture evolution. J. Metamorph. Geol. 22, 159–177.
Lombardo, B., Nervo, R., Compagnoni, R., Messiga, B., Kienast, J.R., Mevel, C., Fiora, L., Piccardo, G., Lanza, R., 1978. Osservazioni preliminari sulle ofioliti metamorfiche del Monviso (Alpi occidentali). Rend. Soc. Ital. Mineral. Petrol. 34, 253–305.
Marot, M., Monfret, T., Pardo, M., Ranalli, G., Nolet, G., 2012. An intermediate-depth tensional earthquake (MW 5.7) and its aftershocks within the Nazca slab, central Chile: a reactivated outer rise fault? Earth Planet. Sci. Lett. 327–328, 9–16.
McAdoo, D.C., Martin, C.F., 1984. Seasat observations of lithospheric flexure seaward of trenches. J. Geophys. Res. 89 (B5), 3201–3210.
McDonough, W.F., 1990. Constraints on the composition of the continental lithospheric mantle. Earth Planet. Sci. Lett. 101, 1–18.
McDonough, W.F., Sun, S.S., 1995. The composition of the Earth. Chem. Geol. 120, 223–253.
Miller, S.A., van der Zee, W., Olgaard, D.L., Connolly, J.A.D., 2003. A fluid-pressure feedback model of dehydration reactions: experiments, modelling, and application to subduction zones. Tectonophysics 370, 241–251.
Oncken, O., the ANCORP working group, 1999. Seismic reflexion image revealing offset of Andean subduction zone earthquakes into oceanic mantle. Nature 397, 341–344.
Padron-Navarta, J.A., Tommasi, A., Garrido, C.J., Sánchez-Vizcaíno, V.L., Gómez-Pugnaire, M.T., Jabaloy, A., Vauchez, A., 2010. Fluid transfer into the wedge controlled by high-pressure hydrofracturing in the cold top-slab mantle. Earth Planet. Sci. Lett. 297, 271–286.
Peacock, S.M., 2001. Are the lower planes of double seismic zones caused by serpentine dehydration in subducting oceanic mantle? Geology 29, 299–302.
Peacock, S.M., Hyndman, R.D., 1999. Hydrous minerals in the mantle wedge and the maximum depth of subduction thrust earthquakes. Geophys. Res. Lett. 26 (16), 2517–2520.
Plunder A., Agard P., Dubacq B., Chopin C., Bellanger M., 2012. How continuous and precise is the record of *P–T* paths? Insights from combined thermobarometry and thermodynamic modelling into subduction dynamics (Schistes Lustrés, W. Alps). J. Metamorph. Geol., 30, 223–246.
Poli, S., Schmidt, M.W., 2002. Petrology of subducted slabs. Ann. Rev. Earth Planet. Sci. 30, 207–235.
Poliakov, A.N.B., Podladchikov, Y., Talbot, C., 1993. Initiation of salt diapirs with frictional overburdens – numerical experiments. Tectonophysics 228, 199–210.
Ranalli, G., Murphy, D.C., 1987. Rheological stratification of the lithosphere. Tectonophysics 132, 281–295.
Ranero, C.R., Phipps Morgan, J., McIntosh, K., Reichert, C., 2003. Bending-related faulting and mantle serpentinization at the Middle America trench. Nature 425, 367–373.
Ranero, C.R., Von Huene, R., 2000. Subduction erosion along the Middle America convergent margin. Nature 404, 748–752.
Rietbrock, A., Waldhauser, F., 2004. A narrowly spaced double-seismic zone in the subducting Nazca plate. Geophys. Res. Lett. 31 (10), L10608.
Rüpke, L.H., Morgan, J.P., Hort, M., Connolly, J.A.D., 2004. Serpentine and the subduction zone water cycle. Earth Planet. Sci. Lett. 223, 17–34.
Schmidt, M.W., Poli, S., 1998. Experimentally based water budgets for dehydrating slabs and consequences for arc magma generation. Earth Planet. Sci. Lett. 163, 361–379.
Schwartz, S., Allemand, P., Guillot, S., 2001. Numerical model of the effect of serpentinites on the exhumation of eclogitic rocks: insights from the Monviso ophiolitic massif (Western Alps). Tectonophysics 342, 193–206.
Shea, W.T., Kronenberg, A.K., 1992. Rheology and deformation mechanisms of an isotropic mica schist. J. Geophys. Res. 97 (B11), 15201–15237.
Singh, S.C., Carton, H., Tapponnier, P., Hananto, N.D., Chauhan, A.P.S., Hartoyo, D., Bayly, M., Moeljopranoto, S., Bunting, T., Christie, P., Lubis, H., Martin, J., 2008. Seismic evidence for broken oceanic crust in the 2004 Sumatra earthquake epicentral region. Nat. Geosci. 1, 777–781.
Singh, S.C., Hananto, N., Mukti, M., Robinson, D.P., Das, S., Chauhan, A., Carton, H., Gratacos, B., Midnet, S., Djajadihardja, Y., Harjono, H., 2011. Aseismic zone and earthquake segmentation associated with a deep subducted seamount in Sumatra. Nat. Geosci. 4, 308–311.
Toda, S., Stein, R.S., Kirby, S.H., Bozkurt, S.B., 2008. A slab fragment wedged under Tokyo and its tectonic and seismic implications. Nat. Geosci. 1, 771–776.
van Keken, P.E., 2003. The structure and dynamics of the mantle wedge. Earth Planet. Sci. Lett. 215, 323–338.
van Keken, P.E., Hacker, B.R., Syracuse, E.M., Abers, G.A., 2011. Subduction factory: 4. Depth-dependent flux of H_2O from subducting slabs worldwide. J. Geophys. Res. 116 (B1), B01401.
Vitale-Brovarone, A., Beltrando, M., Malavieille, J., Giuntoli, F., Tondella, E., Groppo, C., Beyssac, O., Compagnoni, R., 2011. Inherited ocean–continent Transition zones in deeply subducted terranes: insights from Alpine Corsica. Lithos 124, 273–290.
Wada, I., Wang, K., He, J., Hyndman, R.D., 2008. Weakening of the subduction interface and its effects on surface heat flow, slab dehydration, and mantle wedge serpentinization. J. Geophys. Res. 113 (B4), B04402.
Wang, K., Bilek, S., 2011. Do subducting seamounts generate or stop large earthquakes? Geology 39, 819–822.
Warren, C.J., Beaumont, C., Jamieson, R.A., 2008. Modelling tectonic styles and ultra-high pressure (UHP) rock exhumation during the transition from oceanic subduction to continental collision. Earth Planet. Sci. Lett. 267, 129–145.
Watts, A.B., Bodine, J.H., Steckler, M.S., 1980. Observations of flexure and the state of stress in the oceanic lithosphere. J. Geophys. Res. 85 (B11), 6369–6376.
Workman, R.K., Hart, S.R., 1995. Major and trace element composition of the depleted MORB mantle (DMM). Earth Planet. Sci. Lett. 231, 53–72.
Yamato, P., Agard, P., Burov, E., Le Pourhiet, L., Jolivet, L., Tiberi, C., 2007. Burial and exhumation in a subduction wedge: mutual constraints from thermomechanical modeling and natural P–T–t data (Schistes Lustres, western Alps). J. Geophys. Res. Solid Earth 112 (B7).
Zhang, J., Green, H.W., Bozhilov, K., Jin, Z., 2004. Faulting induced by precipitation of water at grain boundaries in hot subducting oceanic crust. Nature 428, 633–636.